Preliminary Trials of Trackerless Augmented Reality in Endoscopic Endonasal Surgery

Yamid Espinel, Nalick Lombion, Luce Compagnone, Nicolas Saroul, Adrien Bartoli

DIA2M, DRCI, CHU de Clermont-Ferrand, 28 Place Henri Dunant, 63000, Clermont-Ferrand, France.

Abstract

Purpose. We present a novel method for augmented reality in endoscopic endonasal surgery. Our method does not require the use of external tracking devices and can show hidden anatomical structures relevant to the surgical intervention.

Methods. Our method registers a preoperative 3D model of the nasal cavity to an intraoperative 3D model by estimating a scaled-rigid transformation. Registration is based on a two-stage ICP approach on the reconstructed nasal cavity. The hidden structures are then transferred from the preoperative 3D model to the intraoperative one using the estimated transformation, projected and overlaid into the endoscopic images to obtain the augmented reality.

Results. We performed qualitative and quantitative validation of our method on 12 clinical cases. Qualitative results were obtained from an ENT surgeon from visual inspection of the hidden structures in the augmented images. Quantitative results were obtained by measuring a target registration error using a novel transillumination-based approach. The results show that the hidden structures of interest are augmented at the expected locations in most cases.

Conclusion. Our method was able to augment the endoscopic images in a sufficiently precise manner when the intraoperative nasal cavity did not deform considerably with respect to its preoperative state. This is a promising step towards trackerless augmented reality in endonasal surgery.

Keywords: Augmented Reality, Endoscopy, Endonasal Surgery, ENT Surgery

1 Introduction

Endoscopic Endonasal Surgery (EES) is the standard surgical approach for the sinonasal tract. Owing to the narrowness and the complexity of the operating area, there is a high risk of damaging structures including the orbits, the optic nerves, the carotid arteries, and the brain. Computer-assisted surgery mitigates such risks by aiding navigation in real-time. Existing approaches are Augmented Virtuality (AV) and Augmented Reality (AR), which both rely on a preoperative CT. The AV approach works by visualising, within the preoperative CT on a secondary display, the tip of a surgical instrument as it explores the nasal cavity. In contrast, the AR approach transfers segmented anatomical structures from the preoperative CT to overlay the endoscopic video display. Existing AV methods [1, 2] and AR methods [3–5] in EES share two technical similarities. First, they require a 3D tracker, whether optical or electromagnetic. In AV, the tracker tracks the surgical instrument; in AR, the tracker tracks the endoscope. Second, they both require the tracker base to be registered to the preoperative CT. However, existing AV and AR methods differ in their state of development: while AV systems are commercially available, including Collin Medical's ENT Surgical Navigation System [6], Medtronic's Fusion ENT Navigation System [7], and Brainlab's Kick EM [8], AR in EES only exists as publicly unavailable research systems. The AV and AR approaches have different drawbacks, owing to the fundamentally different concepts subtending them. The AV approach's main drawback is information splitting on two displays, namely the endoscopic video feed and the preoperative CT, that the surgeon cannot look at simultaneously. This drawback cannot be alleviated as it is part of the AV concept. The AR approach's main drawback is the requirement to prepare the preoperative CT by segmenting the anatomical structures of interest prior to surgery. This drawback is alleviated by modern machine learning CT segmentation techniques. Lastly, the existing AV and AR methods depend on a 3D tracker which may be expensive and inaccurate [9, 10]. Registering the tracker base to the CT is a complex operation which may also incur inaccuracy.

We propose a novel AR method for EES, which uses the image contents to solve for the preoperative CT to endoscope registration. Hence, it does not use a 3D tracker, eliminating this special equipment from the setup. It is thus compatible with the standard operating theatre endoscopes and endoscopic displays. Although our method shares similarities with existing AR approaches applied to other parts of the anatomy [11, 12], it represents the first trackerless method applied to EES. We performed a postoperative trial of our method on 7 patient cases, including 7 left and 5 right nasal cavities. We present expert evaluation on the 12 cavities, visual results for 3 cavities and quantitative results for 1 cavity, using a novel validation protocol.

2 Methodology

The proposed AR method works in four steps, illustrated in figure 1. Step 1 is performed preoperatively. It consists in reconstructing preoperative 3D models of the visible and hidden anatomical structures from the CT data. The visible structure corresponds to the nasal mucosa and will be used to solve registration. The hidden structures of interest depend on the planned procedure. For example, displaying the

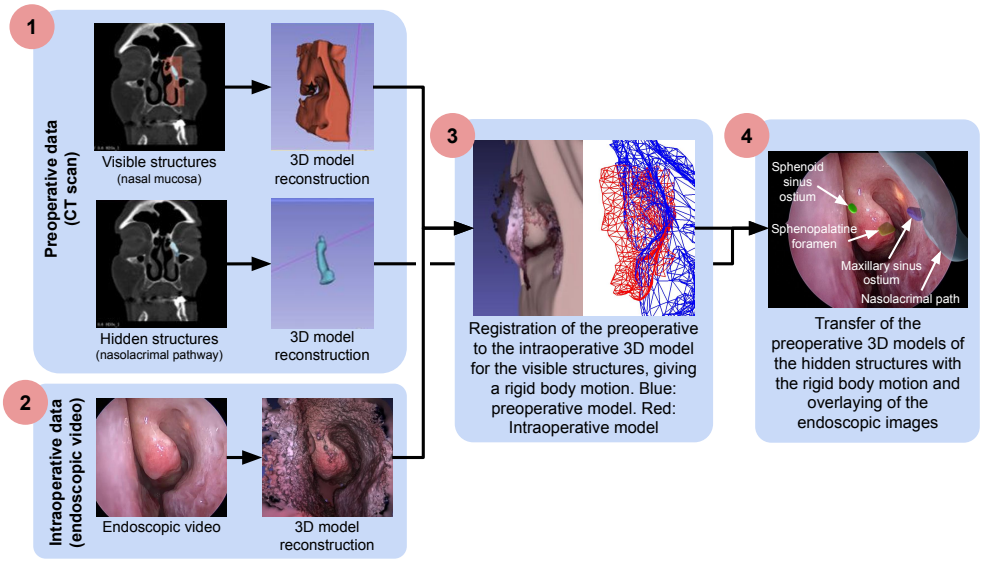

Fig. 1: Pipeline of the four-step proposed AR method in EES. In the first step, the preoperative 3D models of the visible and hidden structures are reconstructed from CT data. In the second step, the intraoperative 3D model of the nasal cavity is reconstructed using SfM. In the third step, the preoperative 3D models are registered to the intraoperative 3D model using ICP. In the fourth step, the registered 3D models of the hidden structures are overlaid on the endoscopic images to achieve AR.

nasolacrimal path is relevant in dacryocystorhinostomy procedures [13], the sphenoid sinus ostium is relevant in sphenoidotomy procedures [14], the sphenopalatine foramen is relevant in sphenopalatine artery ligation procedures [15], and the maxillary sinus ostium is relevant in maxillary antrostomy procedures [16]. Technically, we use 3D Slicer [17], which reconstructs 3D models expressed in CT coordinates. The nasolacrimal path, the maxillary sinus, the sphenoid sinus ostium, and the sphenopalatine foramen were segmented by using the *Draw* and *Fill* between slices tools in all orthogonal planes. The visible model, corresponding to the nasal mucosa, was segmented first by using the *Draw* tool to delimit the boundaries of a 3D block that includes the nasal wall, the middle and inferior turbinates, the roof of the nasal cavity, the sphenoid sinus, the choanal arc and the higher part of the nasopharynx. Then, a second temporary segmentation that selects the air inside the nasal cavity was obtained by using the *Threshold* tool. By subtracting the latter from the original 3D block, the final 3D model of the nasal cavity was obtained. Step 2 is performed intraoperatively, at the beginning of surgery. It consists in reconstructing an intraoperative 3D model of the nasal cavity from the endoscopic images using Structure-from-Motion (SfM), which will be used to solve registration. For that, we film a checkerboard pattern to be used for camera calibration and then the nasal cavity up to the choanal arc. Technically, we use Metashape [18]. This both calibrates the camera and reconstructs the nasal cavity and the endoscope's pose, all expressed in endoscope coordinates. Step

3 registers the CT coordinates to the endoscope coordinates, in two stages. First, we perform an initial rough registration with Absolute Orientation (ABSOR) by selecting a few point correspondences between the preoperative and intraoperative 3D models. These points belong to easily identifiable distinctive structures, including the inferior turbinate, the middle turbinate, and the choanal arc. Second, we refine the registration with the Iterative Closest Point algorithm (ICP). Technically, we use Meshlab [19] for both stages, which provides a rigid body motion aligning the CT to the endoscope coordinates. After the scaled-rigid registration, we obtain values for rotation, translation, and scale factor. The scale factor represents the ratio between the actual intraoperative 3D model scale and metric units. Step 4 uses the rigid body motion to transfer the hidden structures reconstructed in the CT in step 1 to endoscope coordinates and projects them to the endoscopic images to realise the AR overlay. Technically, we use a custom Python script that loads the preoperative and intraoperative data and blends the registered 3D models of the hidden structures with the endoscopic images using Open3D [20]. The proposed method realises augmented reality on the images used to reconstruct the intraoperative 3D model, allowing one to obtain functional augmented reality on the image sequence.

3 Experimental Results

We conducted a prospective non-interventional monocentric study at the Centre Hospitalier Universitaire of Clermont-Ferrand, France. We collected data from 7 patients, for which the nasal mucosa, the nasolacrimal path, the sphenoid sinus ostium, the sphenopalatine foramen, and the maxillary sinus ostium were reconstructed from the preoperative CT scans. A total of 14 cavities were recorded; 7 left and 5 right cavities were reconstructed. A reconstruction is considered successful if it includes at least two of the distinctive structures defined in section 2. Finally, registrations were made using all the intraoperative reconstructions, and AR was rendered. It is worth noting that, although most of the intraoperative models had the same shape as the preoperative models, some of the reconstructions present slight deformations, due to dilating agents being used on those patients.

3.1 Qualitative Evaluation

An ENT surgeon graded the 12 AR cases as 7 *very likely*, 2 *likely*, and 3 *failure*, according to the locations of the hidden structures in the augmented video. We show screenshots for all the 12 cases in figure 2. The cases evaluated as *very likely* show the hidden structures at the expected locations by the surgeon. For example, the nasolacrimal path and the maxillary sinus ostium are located inside the nasal wall, close to the beginning of the middle turbinate, and the sphenopalatine foramen and the sphenoid sinus ostium are close to the posterior end of the middle turbinate. The *likely* cases were mainly due to deformations of the nasal cavity between the preoperative and intraoperative states, making the surgeon doubt about the locations of the inner structures. For example, in Case #2, the structures appear a bit closer than expected to the surgeon. In Case #7, the middle turbinate is surrounded by polyps, making it

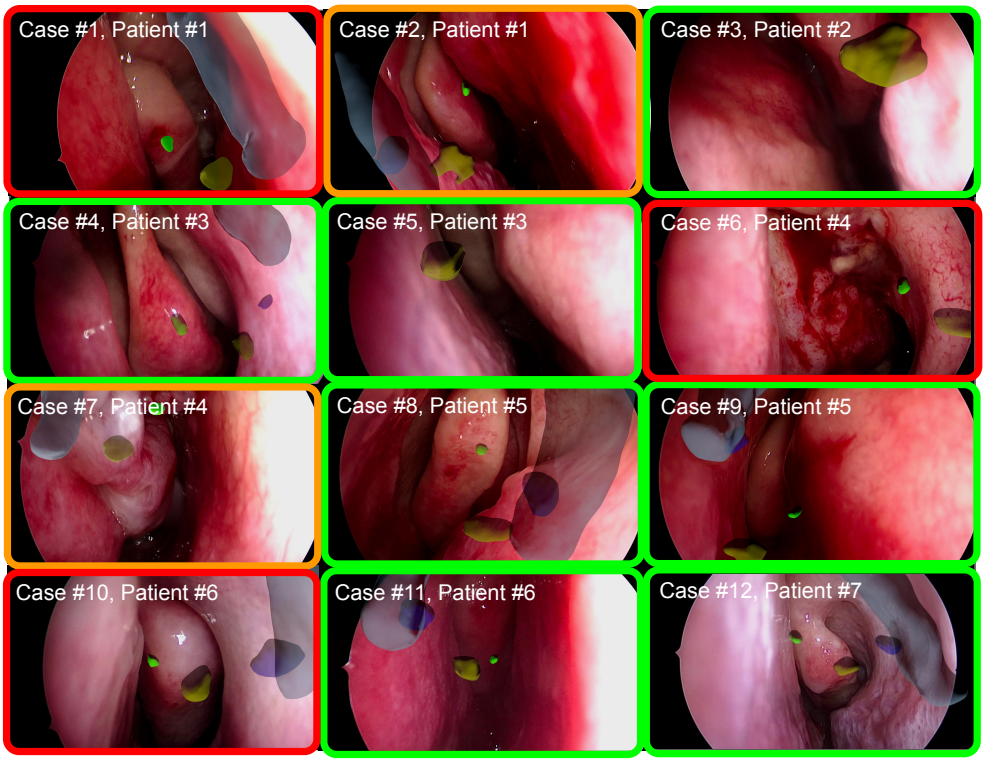

Fig. 2: Screenshots of AR in EES for the 12 evaluated cases. The nasolacrimal path is shown in gray. The maxillary sinus ostium is shown in purple. The sphenopalatine foramen is shown in yellow. The sphenoid sinus ostium is shown in green. The cases evaluated by the ENT surgeon as *very likely* are surrounded in green. The cases evaluated as *likely* are surrounded in orange. The cases evaluated as *failure* are surrounded in red.

difficult to asses the location of the structures. The *failure* cases were also due to deformations of the nasal cavity between the preoperative and intraoperative states, making the structures to appear out of place. For example, in Case #1, the nasolacrimal path appears outside the nasal cavity. In Case #6, the sphenopalatine foramen and the sphenoid sinus ostium do not seem to be behind the middle turbinate. In Case #10, the structures appear very close to the camera, showing the nasolacrimal path outside of the nasal cavity. These deformations were mainly caused by the dilating agents used to increase the space inside the cavity. We have included a video showcasing examples of AR in EES on 3 image sequences.

3.2 Quantitative Evaluation

We performed quantitative assessment on Case #12, which was also evaluated as *very likely* by the medical ENT expert. We used transillumination of the nasolacrimal path

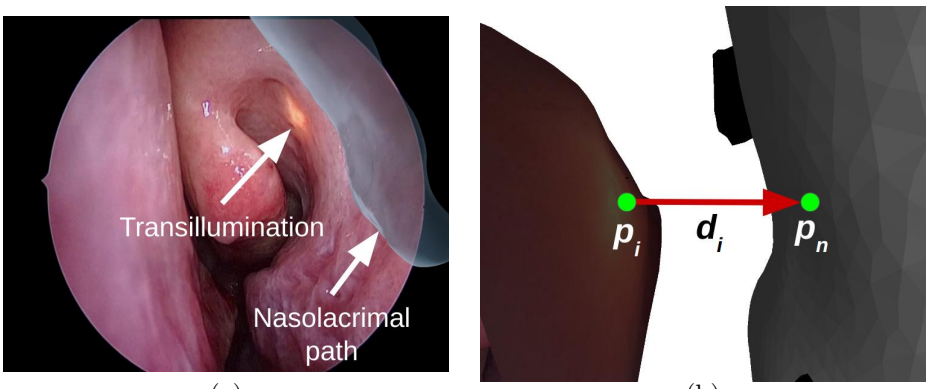

(a) (b)

Fig. 3: Quantitative assessment of AR in EES. (a) Transillumination of the nasolacrimal path and overlay of the registered 3D model. (b) Representation of the distance d_i between a point p_i in the illuminated region of the intraoperative 3D model and the closest point p_n in the nasolacrimal path.

as a reference to measure the target registration error (TRE) as shown in figure 3, due to a lack of distinguishable landmarks in both the preoperative and intraoperative images that could be precisely located and used to measure TRE. Transillumination is used in dacryocystorhinostomy procedures to check for stenosis of the lacrimal duct, which also indicates its location in the nasal cavity. This is done at the beginning of the surgery by inserting a light through the eye lacrymal duct until the light becomes visible inside the nasal cavity. The illuminated area was not used for registration, allowing us to estimate a TRE. Because the nasolacrimal path is located at a distance d_p from the nasal wall, we measured the registration error as TRE $= |d_i - d_p|$, where d_i is the distance between the intraoperative nasal wall and the preoperative nasolacrimal path, and d_p is the distance between the preoperative nasal wall and the nasolacrimal path. We cope with the scale difference between the preoperative and intraoperative models by transforming the intraoperative model back to the preoperative reference frame, giving a TRE in mm. We measure $d_i = \|p_i - p_n\|$ by first hand-picking a point p_i in the illuminated region of the transformed intraoperative nasal wall and then finding the closest point p_n to p_i in the preoperative nasolacrimal path. We measure $d_p = \|p_p - p_n\|$ by finding the closest point p_p to p_i in the preoperative nasal wall. TRE was measured postoperatively. We obtained $d_i = 1.82$ mm and $d_p = 1.92$ mm, giving a satisfying TRE of 0.1 mm.

4 Conclusion

We have shown promising results of AR in EES without using an expensive 3D tracker as in previous work. Our preliminary tests were obtained postoperatively. We plan to 1) extend the quantitative validation of our method on more clinical cases by collecting data from dacryocystorhinostomy procedures and using the proposed novel validation method based on transillumination, 2) test our method intraoperatively,

which will improve intraoperative reconstruction by simply repeating image acquisition and allow live AR, 3) conduct an initial clinical feasibility study involving multiple ENT surgeons, and 4) take the possible deformations into account for registration.

5 Compliance with Ethical Standards

Yamid Espinel declares to have no potential conflicts of interest. Nalick Lombion declares to have no potential conflicts of interest. Luce Compagnone declares to have no potential conflicts of interest. Nicolas Saroul declares to have no potential conflicts of interest. Adrien Bartoli declares to have no potential conflicts of interest.

All procedures involving human participants were in accordance with the ethical standards of the institutional and/or national research committee and with the 1964 Helsinki declaration and its later amendments or comparable ethical standards. This study is also supported by an ethical approval with ID IRB00008526-2020-CE95, issued by CPP Sud-Est VI in Clermont-Ferrand, France.

Informed consent was obtained from the patients included in the study.

References

[1] Mosges, R., Klimek, L.: Computer-assisted surgery of the paranasal sinuses. The Journal of otolaryngology **22**(2), 69–71 (1993)

[2] Vicaut, E., Bertrand, B., Betton, J.-L., Bizon, A., Briche, D., Castillo, L., Lecanu, J.-B., Lindas, P., Lombard, B., Malard, O., Merol, J.-C., Monteyrol, P.-J., Nasser, T., Navailles, B., Prulière-Escabasse, V., Stringini, R., Verillaud, B.: Use of a navigation system in endonasal surgery: Impact on surgical strategy and surgeon satisfaction. a prospective multicenter study. European Annals of Otorhinolaryngology, Head and Neck Diseases **136**(6), 461–464 (2019)

[3] Winne, C., Khan, M., Stopp, F., Jank, E., Keeve, E.: Overlay visualization in endoscopic ent surgery. International Journal of Computer Assisted Radiology and Surgery **6**(3), 401–406 (2011) https://doi.org/10.1007/s11548-010-0507-7

[4] Citardi, M.J., Agbetoba, A., Bigcas, J.-L., Luong, A.: Augmented reality for endoscopic sinus surgery with surgical navigation: a cadaver study. International Forum of Allergy & Rhinology **6**(5), 523–528 (2016) https://doi.org/10.1002/alr.21702

[5] Linxweiler, M., Pillong, L., Kopanja, D., Kühn, J.P., Wagenpfeil, S., Radosa, J.C., Wang, J., Morris, L.G.T., Al Kadah, B., Bochen, F., Körner, S., Schick, B.: Augmented reality-enhanced navigation in endoscopic sinus surgery: A prospective, randomized, controlled clinical trial. Laryngoscope Investigative Otolaryngology **5**(4), 621–629 (2020)

[6] Collin Medical: ENT Surgical Navigation System. https://www.collinmedical.fr/en/collin-navigation-solutions/4554-collin-navigation-solution.html. [Online;

accessed 11-January-2024] (2024)

[7] Medtronic: Fusion ENT Navigation System. https://www.medtronic.com/ca-en/healthcare-professionals/products/ear-nose-throat/image-guided-surgery/fusion-ent-navigation-system.html. [Online; accessed 11-January-2024] (2024)

[8] Brainlab: Kick EM. https://www.brainlab.com/surgery-products/overview-ent-products/ent-navigation-application/. [Online; accessed 11-January-2024] (2024)

[9] Bimedis: Surgical navigation systems for sale. https://bimedis.com/search/search-items/operating-room-surgical-navigation-systems?maincategory=113303. [Online; accessed 11-January-2024] (2024)

[10] J.V. Clarke, A.C.N. A.H. Deakin, Picard, F.: Measuring the positional accuracy of computer assisted surgical tracking systems. Computer Aided Surgery **15**(1-3), 13–18 (2010) https://doi.org/10.3109/10929081003775774

[11] Cheema, M.N., Nazir, A., Sheng, B., Li, P., Qin, J., Kim, J., Feng, D.D.: Image-aligned dynamic liver reconstruction using intra-operative field of views for minimal invasive surgery. IEEE Transactions on Biomedical Engineering **66**(8), 2163–2173 (2019)

[12] Collins, T., Pizarro, D., Gasparini, S., Bourdel, N., Chauvet, P., Canis, M., Calvet, L., Bartoli, A.: Augmented reality guided laparoscopic surgery of the uterus. IEEE Transactions on Medical Imaging **40**(1), 371–380 (2021) https://doi.org/10.1109/TMI.2020.3027442

[13] Ullrich, K., Malhotra, R., Patel, B.: Dacryocystorhinostomy, (2021)

[14] Duan, H.-G., Ji, F., Yuan, H., Wang, H.-L., Chen, M., Ma, D.-J.: Modified sphenoidotomy for isolated sphenoid sinus disease: A series of 117 cases. Science Progress **106**(3) (2023) https://doi.org/10.1177/00368504231189538

[15] Snyderman, C.H., Goldman, S.A., Carrau, R.L., Ferguson, B.J., Grandis, J.R.: Endoscopic sphenopalatine artery ligation is an effective method of treatment for posterior epistaxis. American Journal of Rhinology **13**(2), 137–140 (1999) https://doi.org/10.2500/105065899782106805

[16] Kennedy, D.W., Adappa, N.D.: Endoscopic maxillary antrostomy: Not just a simple procedure. The Laryngoscope **121**(10), 2142–2145 (2011) https://doi.org/10.1002/lary.22169

[17] Slicer: 3D Slicer. https://www.slicer.org/. [Online; accessed 11-January-2024] (2024)

[18] Agisoft: Metashape. https://www.agisoft.com/. [Online; accessed 11-January-2024] (2024)

[19] Cignoni, P., Callieri, M., Corsini, M., Dellepiane, M., Ganovelli, F., Ranzuglia, G.: MeshLab: an Open-Source Mesh Processing Tool. In: Scarano, V., Chiara, R.D., Erra, U. (eds.) Eurographics Italian Chapter Conference. The Eurographics Association, ??? (2008). https://doi.org/10.2312/LocalChapterEvents/ItalChap/ItalianChapConf2008/129-136

[20] Zhou, Q.-Y., Park, J., Koltun, V.: Open3D: A modern library for 3D data processing. arXiv:1801.09847 (2018)